Gallium oxide assisting Ag-loaded calcium titanate photocatalyst for carbon dioxide reduction with water

Hongxuan Qiu,[a] Akira Yamamoto,[a,b] and Hisao Yoshida[a,b*]

[a] *Graduate School of Human and Environmental Studies, Kyoto University, Kyoto 606-8501, Japan*

[b] *Kyoto University, Elements Strategy Initiative for Catalysts and Batteries (ESICB), Kyoto 615-8520, Japan*

* yoshida.hisao.2a@kyoto-u.ac.jp

ABSTRACT

Efficient and highly selective photocatalytic conversion of carbon dioxide (CO_2) into valuable chemicals such as carbon monoxide (CO) using water (H_2O) as an electron donor has been much attractive and deeply desired, which requires development of advanced photocatalysts based on a functional design. Since Ag-loaded calcium titanate ($CaTiO_3$, CTO) photocatalyst showed a high selectivity to CO_2 reduction in aqueous solution and Ag-loaded gallium oxide (Ga_2O_3) photocatalyst showed higher activity for both H_2O splitting and CO_2 reduction, herein, a series of composite photocatalyst samples consisting of Ga_2O_3 and CTO were simply fabricated by calcination of the physical mixtures, followed by loading Ag cocatalyst with a photodeposition method. The optimized sample with Ag cocatalyst exhibited both a high CO formation rate of 56.9 μmol h^{-1} (higher than Ag/Ga_2O_3) and a high selectivity of 95.0 % (comparable to Ag/CTO) in the photocatalytic CO_2 reduction with H_2O. In this composite photocatalyst, most of the electrons generated in the photoexcited Ga_2O_3 part migrated to the minor CTO particles to contribute to the selective CO_2 reduction, which was evidenced by the selective photodeposition of Ag species on the CTO part. The selective CO formation originates from the property of Ag loaded CTO photocatalyst as the active part in the composite photocatalyst. The Ga_2O_3 part functions as an antenna to receive the light and donate the photoexcited electrons to the much-decorated Ag/CTO part, where the concentrated electrons would promote the CO_2 reduction with high efficiency.

Key words: photocatalytic CO_2 reduction, selective Ag loading, antenna function, gallium oxide, calcium titanate composite photocatalyst

1. Introduction

Along with the improvement of our living standards, a large-scale and fast-growth of industrial development has significantly increased the amount of anthropogenic CO_2 as the main component of greenhouse gases in the atmosphere.[1] It has been recognized that the atmospheric CO_2 has

caused global warming and the related climate changes.[2] Till date, artificial photosynthesis has been extensively considered as an ideally potential technology, in which CO_2 would be converted into valuable compounds, such as CO or CH_4.[3-4] It is a state-of-the-art approach to turn waste into treasure by using sustainable solar energy.

In a system of heterogeneous photocatalytic CO_2 reduction by using water as the electron donor, thermodynamically preferable H_2O splitting occurs as a competitive reaction in aqueous solution. Thus, it is significant about how to shift the reaction selectivity from H_2O splitting to CO_2 reduction. The production of CO is preferable as a reduced gaseous product since it is easily separated from aqueous reaction media and very valuable as the raw material in many chemical processes, such as the preparation of syngas[5] or methyl alcohol,[6] and even the industrial reduction of iron oxides.[7] Among substantial metal co-catalysts, silver is widely used as a profound active site for selective CO production.[8] It is true that the moderate loading of Ag nanoparticles (NPs) cocatalyst can effectively raise the selectivity of CO, while the production rate of CO ultimately depends on the photocatalyst itself and has been still insufficient.[9]

As an outstanding wide-band semiconductor (4.7 eV),[10] gallium oxide (Ga_2O_3) has been extensively employed for the investigation of photocatalytic CO_2 reduction, and in many cases it was used after modification.[11] But its selectivity to CO has been low in many cases. For example, Pang et al.[12] reported that Ga_2O_3 loaded by 1 mol% Ag generated 140 μmol h^{-1} CO in a certain condition, albeit the lower selectivity to CO (38.9 %). On the other hand, calcium titanate, ($CaTiO_3$, CTO) has been noticed as one type of indispensable perovskite photocatalysts with a wide-band gap (3.5 eV)[9] owing to its non-toxicity, low-cost, earth-abundant, outstanding chemical stability, and especially appropriate band energy levels for photocatalytic CO_2 reduction.[13-14] By loading Ag cocatalyst, its CO selectivity can reach 96 %, but its yield is only 7.3 μmol h^{-1} in other conditions.[15]

In the present work, we combined these two photocatalyst materials with different properties, Ga_2O_3 of the larger bandgap with high activity and $CaTiO_3$ of lower bandgap with high CO selectivity as a design of a superior photocatalyst exhibiting both high activity and selectivity. Several composite samples consisting of Ga_2O_3 and CTO photocatalysts were fabricated by simple calcination of the physical mixtures. Ag cocatalyst was found to be selectively loaded on the CTO part in a photodeposition method, suggesting the electron transfer from the Ga_2O_3 part to the CTO part. The combination endowed the Ga_2O_3 part with an antenna-like function to receive light and gave the photoexcited electrons to the Ag-loaded CTO part, where the photocatalytic CO_2 reduction took place selectively to form CO. As a result, an advanced photocatalyst exhibiting both high activity and high selectivity was created. Selective photodeposition of Ag species on the specific surface of CTO part supported the electron transfer mechanism.

2. Experimental section

2.1. Preparation of samples

Calcium titanate ($CaTiO_3$, CTO) sample was synthesized by a flux method using stoichiometric amounts of the precursors, $CaCO_3$ (Rare Metallic, 99.9 %) and TiO_2 (rutile, Kojundo, 99.9 %), and a flux reagent, NaCl (Kishida, 99.5 %)[14] at a 1:1 molar ratio of the substrate to the flux. The starting materials (such as 0.037 mol $CaCO_3$ and 0.037 mol TiO_2 with 0.037 mol NaCl) were well mixed in an aluminum mortar in the presence of 5 mL ethanol to make a uniform physical mixture. After that, the mixture was put in an aluminum crucible covered with a lid and heated in an electric muffle furnace at a rate of 200 K h^{-1} up to 1473 K, keeping this temperature for 10 h and then cooled at a rate of 100 K h^{-1} to 773 K, followed by natural cooling to room temperature. The

obtained powder was thoroughly washed with 500 mL of hot water (353 K) for 15 min 3 times to remove residual salt, followed by filtering and drying at 323 K overnight. The sample is referred to as CTO.

The composite samples consisting of Ga_2O_3 and CTO were prepared by a facile thermal treatment method. The total amount of composite samples was 1.0 g with different weight ratios between Ga_2O_3 and CTO. The commercial Ga_2O_3 samples (Kojundo, 99.9%) were physically mixed with CTO and 5 mL ethanol in an aluminum mortar for 20 min 2 times, and then putting them in an aluminum crucible to be calcined at 573, 773, 1073, or 1273 K for 2 h. These samples are referred to as *x*-Ga_2O_3/CTO(*y*), where the *x* means the weight ratio of Ga_2O_3 (wt %) and the *y* is the calcination temperature, like 99-Ga_2O_3/CTO(773). Samples without calcination were also provided, which are shown as *x*-Ga_2O_3+CTO.

Cocatalysts (single metal or dual co-catalysts) were loaded on the surfaces of photocatalysts through a photodeposition (PD) method, in which $AgNO_3$ and $Mn(NO_3)_2$ (Nacalai) were used as the precursors. 1.0 g of the prepared photocatalyst sample was dispersed into 360 mL of ion-exchanged water including required amount of a metal precursor(s) with a bubbling flow of Ar for 1 h in dark conditions to expel air completely. Then the suspension was photoirradiated by a 100 W high-pressure Hg lamp from the center of the vessel for 3 h. All the names of the samples were represented as Ag(PD,*z*)/photocatalyst, where *z* means the loading amount of Ag in wt %, such as Ag(PD,1.0)/*x*-Ga_2O_3/CTO. When two metals, Ag and Mn were involved in the solution simultaneously for depositing 1 wt% loading each, two metals were expected to be deposited and the sample was entitled by Ag(PD,1.0)-Mn(PD,1.0)/*x*-Ga_2O_3/CTO.

Another sample was prepared by using an impregnation method (IMP) to load Ag on the surface of photocatalysts. 1.0 g of the prepared photocatalyst samples was suspended in an aqueous solution (100 mL) of desired amounts of $AgNO_3$ with stirring and heating at 353 K to let the water evaporate, followed by drying at 373 K overnight, and calcined at 573 K for 2 h, which gave Ag(IMP,*z*)/photocatalyst samples.

2.2. Characterization

The crystalline properties of samples were characterized by X-ray diffraction pattern (XRD), which were obtained with a Lab X XRD-6000 (Shimazu) using Cu Kα radiation (40 kV, 30 mA). Diffuse reflectance (DR) UV-vis spectrum was recorded by a V-570 (JASCO). The microstructure and morphology of the samples were observed by a field-emission scanning electron microscopy (SEM; SU-8220, Hitachi, Japan), augmented by energy dispersive X-ray spectroscopy (EDS, 15.0 kV). The accurate loading amount of metal cocatalysts was measured by X-ray fluorescence (XRF) with an EDX-8000 (Shimadzu). Ag K-edge XAFS were obtained by a transmission mode at NW-10A of KEK-PF (Tsukuba, Japan).

2.3. **Photocatalytic reaction**

The photocatalytic CO_2 reduction with H_2O as an electron donor was carried out in an inner-irradiation reaction vessel.[16] The photocatalyst powder (0.3 g) was dispersed in ion-exchanged water (360 mL) containing 1.0 M $NaHCO_3$, and then magnetically stirring in a 30 mL min^{-1} with a bubbling flow of CO_2 without irradiation for 1.0 h. After staring photoirradiation with a 100 W high-pressure Hg lamp, the reaction temperature was 290 K which was controlled by cooling water. The quantity of products in the outlet gas were sampled at each scheduled time and analyzed by using an on-line gas chromatograph (Shimadzu, GC-8A, TCD, Shincarbon ST column, argon carrier). The main products under photoirradiation were limited to CO, H_2 and O_2. Because no other reductive

products than CO and H_2 were observed, the selectivity of CO (S_{co}) is defined as shown in eq. 5. The ratio of the electrons and holes consumed for the gaseous products was calculated by eq. 6.

$S_{CO}(\%)=R_{CO}\times100/(R_{CO}+R_{H2})$ (5)

$R(e^-/h^+)=(R_{CO}+R_{H2})/2R_{O2}$ (6)

where R_{CO}, R_{H2} and R_{O2} are referred to the production rate of CO, H_2 and O_2, respectively.

3. RESULTS AND DISCUSSION

3.1. Photocatalytic performance

Before examining the composite samples, each single photocatalyst loaded by 1.0 wt% Ag in a photodeposition (PD) method, i.e., Ag(PD,1.0)/CTO and Ag(PD,1.0)/Ga_2O_3 samples were evaluated in the photocatalytic CO_2 reduction tests. The results are shown in Figure 1 as 0 and 100 wt% samples, respectively. These single component samples produced CO with the rate of 7.5 and 51.1 μmol h^{-1}, with largely different selectivity to CO of 97.8 and 39.6%, respectively, which were almost consistent with literatures.[17-18] In other words, the Ag-loaded CTO sample can give high CO selectively with low production rates, while the Ag-loaded Ga_2O_3 sample gives mainly H_2 and low CO selectivity with high production rates. Ag cocatalyst on the CTO sample selectively enhanced the photocatalytic activity for CO_2 reduction to produce CO (Table S1, entries 1 and 4), while Ag loading on Ga_2O_3 sample enhanced both H_2 and CO production rates (Table S1, entries 2 and 6).

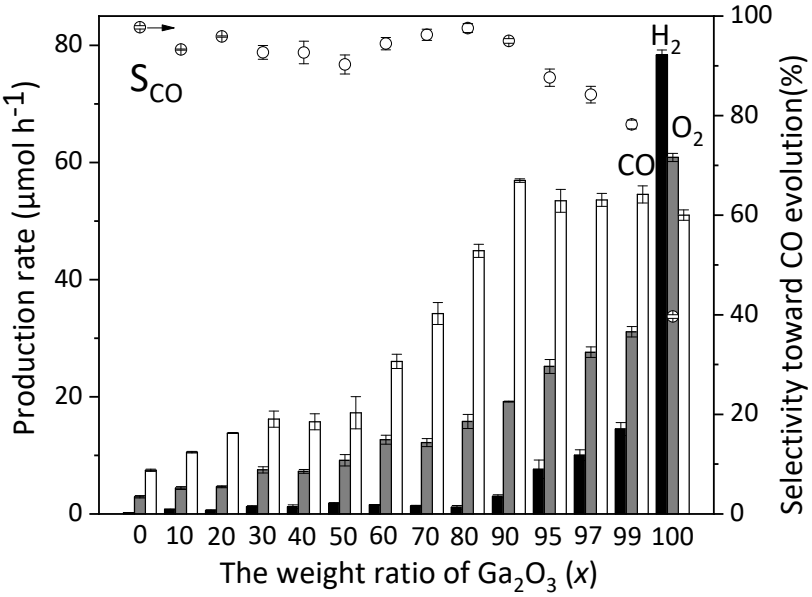

Figure 1. Results of the photocatalytic reaction tests of CO_2 reduction with H_2O over the Ag(PD,1.0)/*x*-Ga_2O_3/CTO(773) samples, in which *x* is the weight ratio of Ga_2O_3 (wt %) and 0 and 100 correspond to not a composite but the single Ag(PD,1.0)/CTO and Ag(PD,1.0)/Ga_2O_3 samples, respectively. Production rates of CO (white bar), H_2 (black bar), O_2 (gray bar) and the selectivity to CO (S_{CO}%, open circles) are shown as an average with error bar for each sample. The data were recorded at 3.5 h after the photoirradiation.

In the cases of the composite photocatalysts with the Ag cocatalyst, all the Ag(PD,1.0)/*x*-

Ga_2O_3/CTO(773) samples in the ratio of x = 10–99 wt%, which were prepared by calcination at 773 K, followed by a photodeposition (PD) method of Ag NPs (1.0 wt%), showed high CO selectivity (Figure 1). The content of Ga_2O_3 (x) in the composite samples much influenced the CO production rate, i.e., CO production increased as Ga_2O_3 increased within the experimental errors. The Ag(PD,1.0)/80-Ga_2O_2/CTO(773) sample gave the highest selectivity (97.6 %) among them, which was nearly same as the Ag(PD,1.0)/CTO sample. The Ag(PD,1.0)/90-Ga_2O_2/CTO(773) sample showed the maximum rate of CO formation (56.9 μmol h^{-1}). Further increasing Ga_2O_3 content (x>90) in the composite sample, corresponding to the decrease of CTO content, the CO production rate did not change dramatically but the CO selectivity decreased. It is notable that the presence of only 1 wt% CTO in the composite Ag(PD,1.0)/99-Ga_2O_3/CTO(773) sample provided much higher CO selectivity than the single Ag(PD,1.0)/Ga_2O_3 sample, meaning that very small amount of CTO drastically varied the photocatalytic property, i.e., the reaction selectivity. Although Ag loading on the Ga_2O_3 gave also high H_2 production as mentioned, all the Ag(PD,1.0)/x-Ga_2O_3/CTO(773) composite samples selectively produced CO and the product distributions were similar to that of not the Ag(PD,1.0)/Ga_2O_3 sample but the Ag(PD,1.0)/CTO sample, which is the most remarkable future of the present composite photocatalysts.

The results of pristine samples without Ag loading were shown in Table S1 entries 1–3. Although the bare CTO generated CO with the production rate of 0.48 μmol h^{-1} about only 55% selectivity for CO and bare Ga_2O_3 has no activity to form CO, the composite material (99-Ga_2O_3/CTO(773)) containing only 1 wt% of CTO could produce CO with nearly ten times higher production rate (5.3 μmol h^{-1}) than that of bare CTO. This suggests that the very minor CTO part in the composite much contributed to the photocatalytic reduction of CO_2.

As for the loading Ag cocatalyst, two methods were examined, the PD method and the impregnation (IMP) method. In the former method, the Ag^+ cations were reduced by the photoexcited electrons to form Ag NPs on the photocatalyst surface. While in the latter method, Ag^+ cations were adsorbed on the surface and deposited by calcination, followed by reduction during the photocatalytic reaction test. Two methods are expected to give different surface distributions, i.e., the PD method deposits Ag NPs on the reductive sites of the photocatalyst surface, while the IMP method forms Ag NPs covering over the surfaces.[19] In this case, the loading method did not give much impact on the CO selectivity for the single CTO and Ga_2O_3 photocatalysts (Table S1, entries 4–7). However, the loading method much influenced the photocatalytic activity of the composite sample; the PD method gave higher CO selectivity than the IMP method, especially on the reaction selectivity (Table S1, entries 8 and 9). Thus, it was noticed that the photoirradiation for loading Ag NPs on the composite has become the key to boosting the photocatalytic CO_2 reduction with H_2O for the CO formation.

A time course of the production rates in the reaction test with the Ag(PD,1.0)/99-Ga_2O_3/CTO(773) sample were recorded and shown in Figure S1. Although the CO production rate slightly decreased and the production rates of O_2 and H_2 gradually increased at the initial period before 3.5 hours, these production rates become constant and continued for the examined 8 hours. Such initial variations followed by successive stabilization in a reaction time course have been reported under similar reaction conditions.[20-21] The initial variation would originate from the variation of the state of the Ag nanoparticles, dissolution of O_2 in the aqueous solution, and so on.[22-23] The Ag NP position stability of the photocatalyst will be mentioned later with Figure S9. The ratio of the electrons and holes consumed for the gaseous products, R (e^-/h^+) became to be 1.0 after the initial

period, indicating that the oxidation of H_2O (eq. 1) and the reduction of CO_2 (eq. 2) and protons (eq. 3) took place simultaneously, where H_2O functioned as a common electron source (eq. 1).

$H_2O + 2\ h^+ \rightarrow 1/2\ O_2 + 2\ H^+$ (1)

$CO_2 + 2\ H^+ + 2\ e^- \rightarrow CO + H_2O$ (2)

$2\ H^+ + 2\ e^- \rightarrow H_2$ (3)

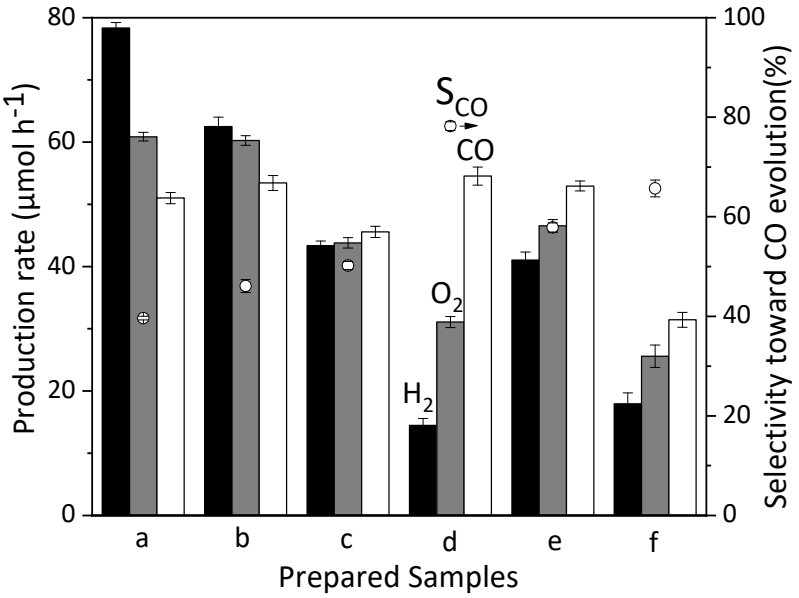

Figure 2. Results of photocatalytic reaction tests of CO_2 reduction with H_2O, production rates of CO (white bar), H_2 (black bar), O_2 (gray bar) and the selectivity to CO (S_{CO}%, open circles) using an average with error bar for each sample, (a) Ag(PD,1.0)/Ga_2O_3, (b) Ag(PD,1.0)/99-Ga_2O_3+CTO, and Ag(PD,1.0)/99-Ga_2O_3/CTO(*y*), where the *y* was (c) 573, (d) 773, (e) 1073, and (f) 1273 K. The data were recorded at 3.5 h after the start of photoirradiation.

As mentioned above, since the Ag(PD,1.0)/99-Ga_2O_3/CTO(773) sample gave enough high CO production yield with moderate CO selectivity among the composite samples (Figure 1), the non-calcined physical mixture consisting of the Ga_2O_3 (99 wt%) and CTO (1 wt%) samples, Ag(PD,1.0)/99-Ga_2O_3+CTO, and the composite samples calcined at various temperatures (*y* K), Ag(PD,1.0)/99-Ga_2O_3/CTO(*y*), were modified by 1.0 wt% Ag cocatalyst in the PD method, and they were examined for the photocatalytic activity tests (Figure 2). The uncalcined physical mixture loaded with Ag cocatalyst (Figure 2b) exhibited photocatalytic activity to form both H_2 and CO similar to that on the Ag(PD,1.0)/Ga_2O_3 sample (Figure 2a), suggesting that 1 wt% physically mixed CTO had no impact on the CO evolution. The calcination of the mixture at a low temperature, 573 K gave less H_2 production and thus the higher CO selectivity was achieved (Figure 2c). This implies that the calcination decreased the H_2 formation property of the mixture sample. Among the calcined samples, the sample calcined at 773 K showed the highest CO selectivity (Figure 2d). The moderate calcination temperature (773 K) would be beneficial for an interaction between Ga_2O_3 and CTO particles without severe change of each property, which was suggested by the unchanged diffraction patterns as mentioned in the Supporting Information (Figure S2c). The highest calcination temperature (1273 K) decreased the photocatalytic activity (Figure 2f), which would be

due to some changes about the properties of both Ga_2O_3 and CTO photocatalysts at high temperature. It was suggested by the change of the diffraction patterns (Figure S2e) and morphologies (Figure S3d).

3.2. Characterization of composite photocatalysts

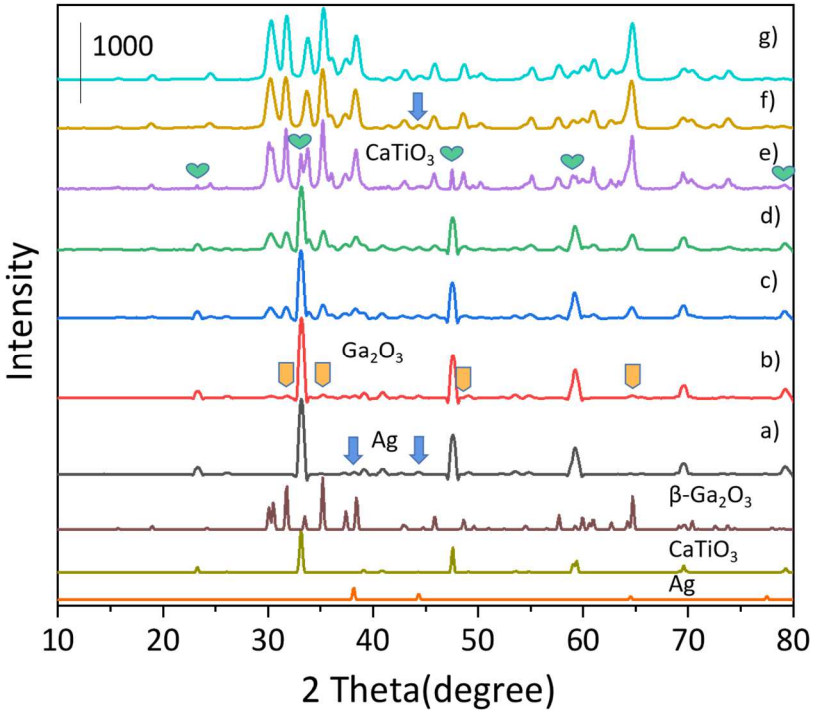

Figure 3. XRD patterns of the single samples, (a) Ag(PD,1.0)/CTO, (g) Ag(PD,1.0)/Ga_2O_3 and the Ag(PD,1.0)/*x*-Ga_2O_3/CTO(773) composite samples, where *x* is (b) 10, (c) 30, (d) 50, (e) 90 and (f) 99 wt%, and the patterns from the ICSD database are also shown in the XRD patterns, ICSD#34243 for β-Ga_2O_3, ICSD#162909 for $CaTiO_3$, and ICSD#44387 for Ag.

The actual loading amount of Ag cocatalyst and contents of Ga_2O_3 in the samples were confirmed by XRF (Table. S2), which were almost the same as the values desired in preparation. Figure 3 shows the XRD patterns of the Ag-loaded samples and ICSD database references. The weak characteristic peaks of Ag (38.2 and 44.6 °) were revealed in the Ag/CTO and Ag/10-Ga_2O_3/CTO samples (Figure 3a and b). Although the strongest peak (38.2 °) was covered with the increase of Ga_2O_3 content (38.4 °), the characteristic peak of Ag (44.6 °) still existed, which proved the real presence of metallic silver. There was observed that the characteristic peaks assignable to Ga_2O_3 (31.8, 35.2, 48.6 and 64.7 °) in the 10-Ga_2O_3/CTO(773) and 30-Ga_2O_3/CTO samples (Figure 3b). Similarly, XRD pattern assigned to $CaTiO_3$ (23.3, 33.1, 47.6, 59.4 and 79.3 °) could be clearly seen for the composites containing 50 and 90 wt% of Ga_2O_3 (Figure 3d and e), but not for the 99-Ga_2O_3/CTO(773) sample due to the small ratio of CTO (Figure 3f). It is noted that no obvious change was observed for the diffraction patterns of Ga_2O_3 and $CaTiO_3$ in these composite samples, meaning no drastic chemical reaction occurred on these original crystal structure of both Ga_2O_3 and CTO when the physical mixture was calcined at 773 K.

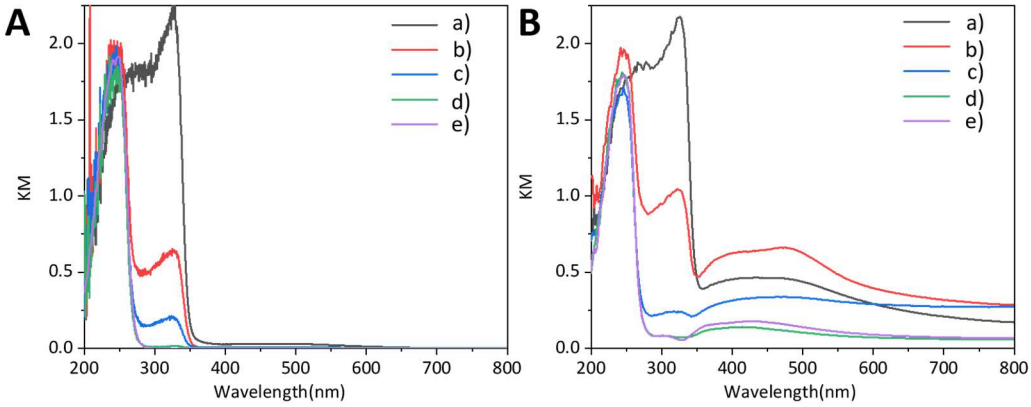

Figure 4. DR UV-vis spectra of [A] the single samples, (a) bare CTO, (e) bare Ga_2O_3, and composites, (b) 50-Ga_2O_3/CTO(773), (c) 90-Ga_2O_3/CTO(773), and (d) 99-Ga_2O_3/CTO(773); [B] the corresponding Ag-loaded samples.

The UV-vis spectra of some bare samples and Ag-loaded samples are shown in Figure 4A and 4B, respectively. Bare CTO exhibited a large absorption band in the range of shorter wavelength than ca. 350 nm, which was consistent with 3.5 eV of the band gap (Figure 4Aa).[17] The bare Ga_2O_3 (Figure 4Ae) showed the band at shorter wavelength than 300 nm, which gave the band gap of 4.7 eV.[10] The 99-Ga_2O_3/CTO(773) sample showed a very weak band assignable to $CaTiO_3$ around 280 to 330 nm (Figure 4Ac) and the 90-Ga_2O_3/CTO(773) sample showed larger intensity due to the larger CTO content (Figure 4Ad). In 50-Ga_2O_3/CTO(773) sample, the intensity of the characteristic absorption peak (280-330 nm) about CTO was not exactly a half but moderate compared to that of bare CTO (Figure 4Ab). These results showed that both the CTO and Ga_2O_3 parts in the composite samples calcined at 773 K had the original optical properties.

The surface plasmon resonance (SPR) band of the Ag nanoparticles from 400 to 500 nm[23] was observed in all the Ag-loaded samples (Figure 4B). The 50-Ga_2O_3/CTO(773) sample (Figure 4Bb) had the evidently higher intensity than the Ag(PD,1.0)/CTO sample (Figure 4Ba). While the Ag(PD,1.0)/99-Ga_2O_3/CTO(773) and Ag(PD,1.0)/90-Ga_2O_3/CTO(773) samples (Figures 4Bc and 4Bd) presented similar curves as the Ag(PD,1.0)/CTO sample with lower intensity. It is noted that the SPR band intensity increased with increasing CTO content in the composite samples although the Ag content was almost the same as shown in Table S2.

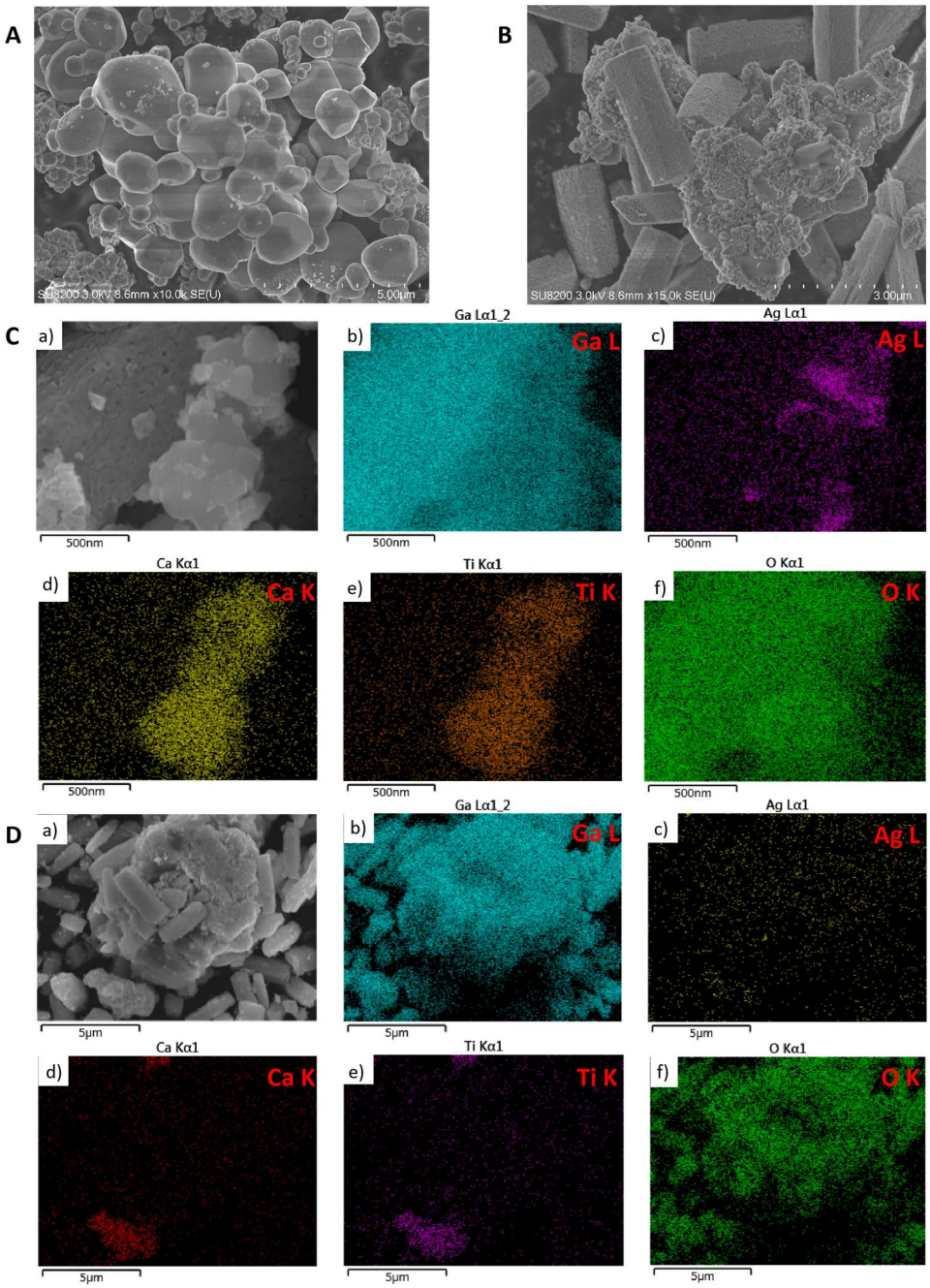

Figure 5. Scanning electron microscopy (SEM) images of the samples, [A] Ag(PD,1.0)/CTO, [B, C] Ag(PD,1.0)/99-Ga_2O_3/CTO(773), and [D] Ag(PD,1.0)/99-Ga_2O_3+CTO, with EDS elemental mappings for the composite samples [C, D].

According to the reaction test results of the uncalcined and calcined samples in Figures 2b and d, the calcination at optimal temperature (773 K) improved the CO selectivity and maintained the same CO yield. In other words, the calcination decreased the H_2 production rate, which was the property of the Ga_2O_3 photocatalyst, meaning that the calcination might take away the photocatalytic activity of the Ga_2O_3 part although it could absorb the light (Figure 4A and B). To explore the main reasons for this fact, energy dispersive X-ray spectroscopy (EDS) was taken for elemental mappings of the prepared samples as shown in Figure 5C and D. In the SEM image of the Ag(PD,1.0)/CTO sample (Figure 5A), compared with bare CTO (Figure S4a), Ag NPs of ca. 50 nm

in size was seen clearly on the surface of the roundish CTO particles (ca. 1.0 μm in size) with a low surface density. In the Ag(PD,1.0)/99-Ga_2O_3/CTO(773) sample (Figure 5B), the roundish CTO particle and the rod-like Ga_2O_3 particles (ca. 2.2 μm in size) seemed to be bound tightly and larger Ag NPs (ca. 70 nm in size) covered on only the CTO surface with a high surface density. According to the EDS mapping (Figure 5C), it was confirmed that Ag NPs were selectively deposited on the CTO surface. Although some white points were observed on the surface of Ga_2O_3 in the SEM image, they were not Ag NPs (Figure 5B and C). Conversely, in the non-calcined physical mixture sample (Figure 5D) where the CTO and Ga_2O_3 particles existed somewhat independently, and Ag NPs were more evenly dispersed on the surfaces of the two components. The chemical states of Ag on the surfaces of the 99-Ga_2O_3/CTO(773) and 99-Ga_2O_3+CTO samples were confirmed by XAFS to be metallic silver (Figure S5), even though they have completely different loading distributions and photocatalytic activities.

It can be seen from Figure 1 that there is a big difference in the photocatalytic CO_2 reduction results of composite materials with different weight ratios. SEM images of four representative samples among them are shown in Figure S6. The composites with different ratios were clearly distinguished from each other in the images based on the morphologies. There was no specific structure such as core-shell structure between CTO and Ga_2O_3, while the two components showed each original roundish and rod-like morphologies and contacted to each other, implying that it enabled electron transfer between the two materials. In the EDS mappings of all these four samples (Figure S7), Ag NPs were found only on the CTO surfaces and the area density of Ag deposited on the surface of CTO gradually increased with the decreasing content of CTO. This suggests that in these composites with different weight ratios, the photoirradiated Ga_2O_3 donated most of the photoexcited electrons to the CTO parts in one direction, and only the surface of the CTO parts was selectively loaded with Ag through the reduction of Ag^+ by the excited electrons in the photodeposition process.

In the composite sample owning less CTO content, the concentration of the deposited Ag NPs on the CTO surface would be denser due to the selective photodeposition. This might be one possible reason for the high activity and selectivity to produce CO. Assuming the Ag NP density of CTO in the Ag(PD,1.0)/99-Ga_2O_3/CTO(773) sample (Figure 5B) would be similar to that on the 10 wt% Ag loaded CTO sample, for comparison, a single Ag(PD,10.0)/CTO sample was prepared for comparison (Figure S8A) and examined in the photocatalytic reaction test (Figure S8B). The photocatalytic activity much decreased compared with the 1.0 wt % Ag loaded sample. It is suggested that the CTO photocatalyst covered with highly deposited Ag NPs cocatalyst could not absorb enough the light (Figure S8C) and thus could not work as photocatalyst efficiently. It means the fact that Ag cocatalyst can much contribute to the selective CO_2 reduction to CO over $CaTiO_3$ photocatalyst. However, the CO production rate was limited due to the limitation of Ag loading amount on the $CaTiO_3$ particles, i.e., covering the $CaTiO_3$ surface with large amount of Ag cocatalyst tends to suppress the photocatalytic activity. In the Ga_2O_3-$CaTiO_3$ composite photocatalyst, the $CaTiO_3$ part was selectively decorated with high surface density of Ag cocatalyst while the Ga_2O_3 part was free from the decoration and these parts are connected to each other. This enabled that the Ga_2O_3 part can receive light like as an antenna and transfer the photoexcited electrons to the much-decorated $CaTiO_3$ part, where selective CO_2 reduction takes place sufficiently.

Several EDS mapping images of other two samples are displayed in Figure S9. After the photocatalytic CO_2 reduction test, the used composite photocatalyst had unchanged morphology

and Ag NPs were still mainly loaded on the CTO surface (Figure S9A). It is reported that Ag NPs on photocatalyst were oxidized and dissolved as Ag^+ and redeposited on the other reductive sites to form or grew Ag NPs during the photoirradiation in the photocatalytic reaction test.[22] In the case of the present composite photocatalyst, the position of Ag NPs seemed unchanged not degraded. When the Ag cocatalyst was loaded by the IMP method, it was confirmed that Ag NPs were located on the entire surface unselectively (Figure S9B). This also verifies the previous results (Table S1, entry 9), i.e., the selective deposition of Ag on this composite photocatalyst by the photodeposition method is significantly important for the photocatalytic activity in the CO_2 reduction (Table S1, entries 8 and 9).

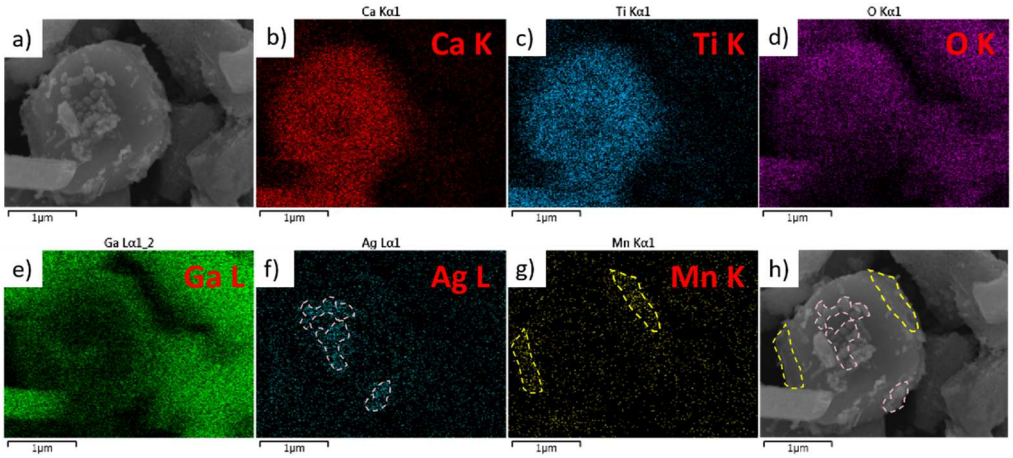

Figure 6. [a] Scanning electron microscopy (SEM) images, [b–g] EDS elemental mappings and [h] outline for Ag–L and Mn–K elements of the Ag(PD,1.0)-Mn(PD,1.0)/99-Ga_2O_3/CTO(773) sample.

Further, a conventional photodeposition test was carried out to determine whether the holes can be transferred between the two components in the 99-Ga_2O_3/CTO(773) sample. One combination of easily reduced and oxidized metals, Ag and Mn, was simultaneously photodeposited on the surface of the composites. Mn species reacted on the oxidation facet of CTO, typically as follows:[24]

$Mn^{2+} + 2\ h^+ + 2H_2O \rightarrow MnO_2 + 4H^+$ (4)

It could be seen from Figure 6 that Ag NPs were still loaded selectively on the surface of CTO (Figure 6f). Meanwhile, Mn with the marginal loading amount (Table S2, entry 8) also had the characteristics of selective loading predominantly on the CTO part. In addition, it is noticed that Mn species was loaded selectively on the different facets of the CTO part from those for Ag species (Figure 6g). It shows that the CTO part had two kinds of facets, and the reduction reaction and oxidation reaction occurred simultaneously on different facets under photoirradiation.[15] These results revealed that the CTO part was the dominant loading center for these dual metal cocatalysts under photoirradiation. Furthermore, a small amount of Mn species was also found on the Ga_2O_3 part. This suggests that there was a certain resistance for the transfer of holes, most of the holes of the Ga_2O_3 could transfer to the CTO part while a small number of holes remained in the Ga_2O_3 part. In summary, the Ga_2O_3 part acted as an antenna to receive the light and transfer most of the generated electrons and the holes to the CTO part.

3.3. Proposed mechanism

The proposed photoabsorption-electron transfer mechanism for the photodeposition of Ag NPs on the Ga_2O_3/CTO composite photocatalyst is shown in Figure 7A. According to the calcination of composite at sufficient temperature (773 K), the good contact between the surfaces of the two components, Ga_2O_3 and CTO particles, was created and allowed electron transfer between them. Since the conduction band (CB) of Ga_2O_3 (−1.3 eV)[25] is more negative than that of CTO (−0.8 eV)[26] as shown in Figure 7B, the most of the excited electrons generated in the Ga_2O_3 part can transfer to the CTO part through the interfaces. In the photodeposition method (Figure 7A), the CTO part received many excited electrons from the Ga_2O_3 part in addition to the originally photogenerated electrons, so that the Ag NPs were selectively loaded on the reductive facets of the CTO part.

Therefore, in this photocatalytic CO_2 reduction reaction (Figure 7C), almost all the electrons and most of the holes generated from photoirradiated Ga_2O_3 part can transfer to the CTO part. The reductive facets of the CTO part loaded with high-density Ag can selectively reduce CO_2 and H^+ to form CO and H_2O (eq. 2), and the blank oxidation facets of the CTO part and the Ga_2O_3 part can oxidize H_2O to O_2 and H^+ (eq. 1). In this advanced composite material, simple physical grinding and effective calcination endowed the Ga_2O_3 part with the function as a kind of antenna, which donated substantial electron-hole pairs from the body through the surface contact with the CTO part that was densely covered by the Ag NPs. The best balance of the two components, the antenna, and the reaction parts, should depend on their particle size and properties; in the present conditions, it would be optimal one about ca. 90 wt% of Ga_2O_3 in the composite photocatalyst, like the 90-Ga2O3/CTO(773) sample. The optimal amount of Ag NPs should be varied with the content of the composites, e.g., it was 1 wt% for the 90-Ga_2O_3/CTO(773) sample and 5 wt% for the 50-Ga_2O_3/CTO(773) sample (Figure S10). Note that the optimized Ag loading would be determined by the ratio to the CTO content, which were 1 and 5 wt% of Ag NPs for 10 and 50 wt% of CTO part, respectively, in the composites.

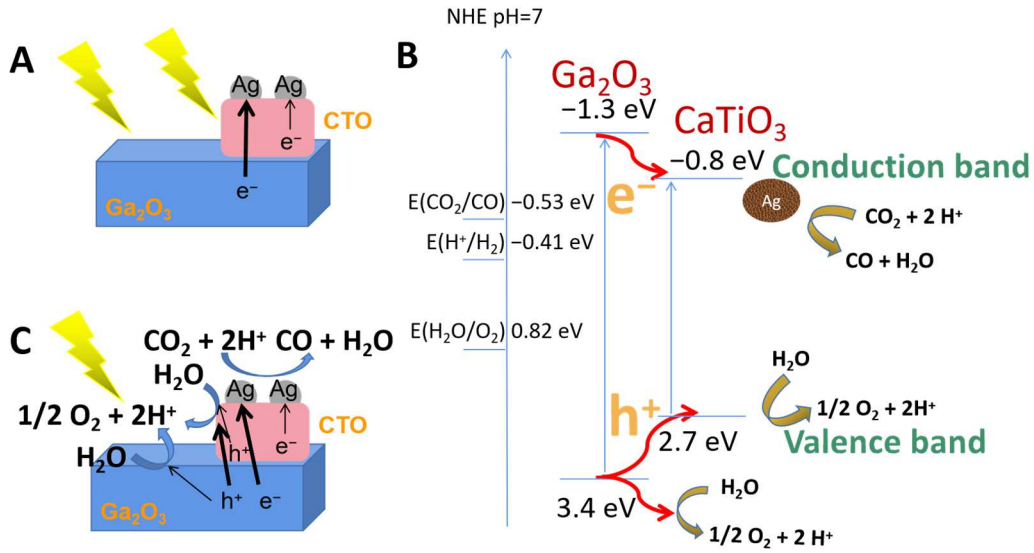

Figure 7. Schematic diagram of [A] the photodeposition method, [B] the band diagram for $CaTiO_3$ and Ga_2O_3, and [C] the photocatalytic CO_2 reduction with H_2O in an Ag-loaded composite photocatalyst.

4. Conclusion

In this paper, we illustrated that the simple physical mixing and effective calcination could create a specific composite photocatalyst containing Ga_2O_3 and $CaTiO_3$, where the Ga_2O_3 part functioned as an antenna to receive the light and donated the excited electrons and holes to the $CaTiO_3$ part decorated with Ag nanoparticle (NP) cocatalyst that acted as an active part for CO_2 reduction with water. Meanwhile the photocatalytic composite sample presented better performance about photocatalytic CO_2 reduction than every individual component sample.

The photodeposition method selectively decorated the $CaTiO_3$ part with the Ag NP cocatalysts to make it become the active center for the photocatalytic CO_2 reduction by using the electrons and holes generated from Ga_2O_3 part. In the optimal Ag(PD,1.0)/90-Ga_2O_3/CTO(773) sample exhibiting high CO yield (56.9 μmol h^{-1}) and high selectivity (95.0 %), the minor $CaTiO_3$ part was well covered with many Ag NP cocatalysts and show high CO selectivity but less ability for photoabsorption while the bare Ga_2O_3 part free from Ag NPs could receive the light to give electrons and holes to the $CaTiO_3$ part like as an antenna.

Although the high concentration of the Ag NP cocatalyst would be intrinsically beneficial for the CO_2 reduction with electrons and protons, we sometimes face the problem that an excess deposition of Ag NP on the photocatalyst surface decreases the photoabsorption and thus suppress the photocatalytic performance. The present results suggest that an antenna part attached to the much decorated active photocatalyst can give the possibility to become the efficient composite photocatalyst. Both effective calcination and selective Ag loading by the PD method were very significant for the successful preparation of this composite. We believe that more promising combination of the antenna and the active part will be found by using simple preparation methods.

Supporting Information

Additional reaction tests, time course of sample, additional material measurements about XRD, SEM, XRF and Ag K-edge XANES, performance evaluation and comparison with the overloaded amount of Ag, additional SEM-EDS images, optimization of the Ag loading amount

Author Contributions

H.Q.: Conceptualization, Investigation, Writing original draft. A.Y.: Investigation, Funding acquisition. H.Y.: Conceptualization, Supervision, Reviewing and Editing manuscript, Funding acquisition.

Notes

The authors declare no competing financial interest.

Acknowledgement

The XAFS spectra of the samples were measured at the NW10A of the Photon Factory (PF) with the approval of the Photon Factory Program Advisory Committee (proposal number 2020G667). This work was financially supported by ISHIZUE 2020 of the Kyoto University Research Development Program, the joint research program of the Artificial Photosynthesis, Osaka City University, a Grant-in-Aid for Scientific Research (B) (21H01975), and a Grant-in-Aid for Challenging Research

(Exploratory, 20K21108) from the Japan Society for the Promotion of Science (JSPS), and the Program for Element Strategy Initiative for Catalysts & Batteries (ESICB, JPMXP0112101003), commissioned by the MEXT of Japan. HQ appreciates the China Scholarship Council providing a scholarship (CSC.202006260014).

References

This article references 26 other publications.

1. Keenan, T. F.; Luo, X.; De Kauwe, M. G.; Medlyn, B. E.; Prentice, I. C.; Stocker, B. D.; Smith, N. G.; Terrer, C.; Wang, H.; Zhang, Y.; Zhou, S., A constraint on historic growth in global photosynthesis due to increasing CO_2. *Nature* **2021,** *600* (7888), 253-258.

2. Vijay, S.; Ju, W.; Brückner, S.; Tsang, S.-C.; Strasser, P.; Chan, K., Unified mechanistic understanding of CO_2 reduction to CO on transition metal and single atom catalysts. *Nature Catalysis* **2021,** *4* (12), 1024-1031.

3. Wang, J.-W.; Jiang, L.; Huang, H.-H.; Han, Z.; Ouyang, G., Rapid electron transfer via dynamic coordinative interaction boosts quantum efficiency for photocatalytic CO_2 reduction. *Nature Communications* **2021,** *12* (1), 4276.

4. Li, J.; Huang, H.; Xue, W.; Sun, K.; Song, X.; Wu, C.; Nie, L.; Li, Y.; Liu, C.; Pan, Y.; Jiang, H.-L.; Mei, D.; Zhong, C., Self-adaptive dual-metal-site pairs in metal-organic frameworks for selective CO_2 photoreduction to CH_4. *Nature Catalysis* **2021,** *4* (8), 719-729.

5. Proietto, F.; Li, S.; Loria, A.; Hu, X.-M.; Galia, A.; Ceccato, M.; Daasbjerg, K.; Scialdone, O., High-pressure synthesis of CO and syngas from CO_2 reduction using Ni–N-doped porous carbon electrocatalyst. *Chemical Engineering Journal* **2022,** *429*, 132251.

6. McGuinness, D. S.; Patel, J.; Amin, M. H.; Bhargava, S. K., DFT Study of Nickel-Catalyzed Low-Temperature Methanol Synthesis. *ChemCatChem* **2017,** *9* (10), 1837-1844.

7. Bernasowski, M., Theoretical Study of the Hydrogen Influence on Iron Oxides Reduction at the Blast Furnace Process. *steel research international* **2014,** *85* (4), 670-678.

8. Iizuka, K.; Wato, T.; Miseki, Y.; Saito, K.; Kudo, A., Photocatalytic Reduction of Carbon Dioxide over Ag Cocatalyst-Loaded $ALa_4Ti_4O_{15}$ (A = Ca, Sr, and Ba) Using Water as a Reducing Reagent. *Journal of the American Chemical Society* **2011,** *133* (51), 20863-20868.

9. Jiang, E.; Yang, L.; Song, N.; Zhang, X.; Liu, C.; Dong, H., Multi-shelled hollow cube $CaTiO_3$ decorated with $Bi_{12}O_{17}Cl_2$ towards enhancing photocatalytic performance under the visible light. *Journal of Colloid and Interface Science* **2020,** *576*, 21-33.

10. Kikkawa, S.; Teramura, K.; Asakura, H.; Hosokawa, S.; Tanaka, T., Development of Rh-Doped Ga_2O_3 Photocatalysts for Reduction of CO_2 by H_2O as an Electron Donor at a More than 300 nm Wavelength. *The Journal of Physical Chemistry C* **2018,** *122* (37), 21132-21139.

11. Yamamoto, M.; Yoshida, T.; Yamamoto, N.; Nomoto, T.; Yamamoto, Y.; Yagi, S.; Yoshida, H., Photocatalytic reduction of CO_2 with water promoted by Ag clusters in Ag/Ga_2O_3 photocatalysts. *Journal of Materials Chemistry A* **2015,** *3* (32), 16810-16816.

12. Pang, R.; Teramura, K.; Tatsumi, H.; Asakura, H.; Hosokawa, S.; Tanaka, T., Modification of Ga_2O_3 by an Ag–Cr core–shell cocatalyst enhances photocatalytic CO evolution for the conversion of CO_2 by H_2O. *Chemical Communications* **2018,** *54* (9), 1053-1056.

13. Anzai, A.; Fukuo, N.; Yamamoto, A.; Yoshida, H., Highly selective photocatalytic reduction of carbon dioxide with water over silver-loaded calcium titanate. *Catalysis Communications* **2017,** *100*, 134-138.

14. Yoshida, H.; Zhang, L.; Sato, M.; Morikawa, T.; Kajino, T.; Sekito, T.; Matsumoto, S.; Hirata, H., Calcium titanate photocatalyst prepared by a flux method for reduction of carbon dioxide with water. *Catalysis Today* **2015,** *251*, 132-139.

15. Soltani, T.; Zhu, X.; Yamamoto, A.; Singh, S. P.; Fudo, E.; Tanaka, A.; Kominami, H.; Yoshida, H., Effect of transition metal oxide cocatalyst on the photocatalytic activity of Ag loaded $CaTiO_3$ for CO_2 reduction with water and water splitting. *Applied Catalysis B: Environmental* **2021,** *286*, 119899.

16. Zhu, X.; Yamamoto, A.; Imai, S.; Tanaka, A.; Kominami, H.; Yoshida, H., Facet-selective deposition of a silver–manganese dual cocatalyst on potassium hexatitanate photocatalyst for highly selective reduction of carbon dioxide by water. *Applied Catalysis B: Environmental* **2020,** *274*, 119085.

17. Soltani, T.; Yamamoto, A.; Singh, S. P.; Anzai, A.; Fudo, E.; Tanaka, A.; Kominami, H.; Yoshida, H., Simultaneous Formation of CO and H_2O_2 from CO_2 and H_2O with a Ag–MnO_x/$CaTiO_3$ Photocatalyst. *ACS Applied Energy Materials* **2021,** *4* (7), 6500-6510.

18. Pang, R.; Teramura, K.; Asakura, H.; Hosokawa, S.; Tanaka, T., Effect of Cr Species on Photocatalytic Stability during the Conversion of CO_2 by H_2O. *The Journal of Physical Chemistry C* **2019,** *123* (5), 2894-2899.

19. Jasso-Salcedo, A. B.; Palestino, G.; Escobar-Barrios, V. A., Effect of Ag, pH, and time on the preparation of Ag-functionalized zinc oxide nanoagglomerates as photocatalysts. *Journal of Catalysis* **2014,** *318*, 170-178.

20. Zhu, X.; Yamamoto, A.; Imai, S.; Tanaka, A.; Kominami, H.; Yoshida, H., Correction: A silver–manganese dual co-catalyst for selective reduction of carbon dioxide into carbon monoxide over a potassium hexatitanate photocatalyst with water. *Chemical Communications* **2020,** *56* (16), 2514-2514.

21. Xu, X.; Asakura, H.; Hosokawa, S.; Tanaka, T.; Teramura, K., Tuning Ag-modified $NaTaO_3$ to achieve high CO selectivity for the photocatalytic conversion of CO_2 using H_2O as the electron donor. *Applied Catalysis B: Environmental* **2023,** *320*, 121885.

22. Pang, R.; Teramura, K.; Asakura, H.; Hosokawa, S.; Tanaka, T., Highly selective photocatalytic conversion of CO_2 by water over Ag-loaded $SrNb_2O_6$ nanorods. *Applied Catalysis B: Environmental* **2017,** *218*, 770-778.

23. Zhu, X.; Anzai, A.; Yamamoto, A.; Yoshida, H., Silver-loaded sodium titanate photocatalysts for selective reduction of carbon dioxide to carbon monoxide with water. *Applied Catalysis B: Environmental* **2019,** *243*, 47-56.

24. Wang, S.; Teramura, K.; Hisatomi, T.; Domen, K.; Asakura, H.; Hosokawa, S.; Tanaka, T., Dual Ag/Co cocatalyst synergism for the highly effective photocatalytic conversion of CO_2 by H_2O over Al-$SrTiO_3$. *Chemical Science* **2021,** *12* (13), 4940-4948.

25. Zheng, X.-Q.; Lee, J.; Rafique, S.; Han, L.; Zorman, C. A.; Zhao, H.; Feng, P. X. L., Ultrawide Band Gap β-Ga_2O_3 Nanomechanical Resonators with Spatially Visualized Multimode Motion. *ACS Applied Materials & Interfaces* **2017,** *9* (49), 43090-43097.

26. Kumar, A.; Navakoteswara Rao, V.; Kumar, A.; Venkatakrishnan Shankar, M.; Krishnan, V., Interplay between Mesocrystals of $CaTiO_3$ and Edge Sulfur Atom Enriched MoS_2 on Reduced Graphene Oxide Nanosheets: Enhanced Photocatalytic Performance under Sunlight Irradiation. *ChemPhotoChem* **2020,** *4* (6), 427-444.